8th World Conference on Experimental Heat Transfer, Fluid Mechanics, and Thermodynamics
June 16-20, 2013, Lisbon, Portugal

Influence of CNFs layer morphology on convective heat transfer behavior

T.J. Taha and T.H. van der Meer

Thermal Engineering, Faculty of Engineering and Technology,

University of Twente, 7500 AE Enschede, Netherlands

E-mail : t.j.taha@utwente.nl

ABSTRACT

In this work, heat transfer surface modification is made by layers of carbon nanofiber (CNF) on 50μm nickel wire using a chemical vapor deposition process (CVD). Three different CNF layer morphologies are made, at 500˚C, 600˚C and 700˚C, to investigate their influence on heat transfer performance characteristics. Moreover, the influence of the CNFs layer thickness on each batch of morphology is studied. Experimental results shows that samples made at 500˚C creates an insulating layer of CNFs, which is attributed to the dense structure of the layer of fibers, resulting in 25% lower heat transfer compared to the heat transfer performance of the bare wire. However, samples made at 600˚C, exhibit relatively open layer of CNFs and lower thermal conductivity compared to samples made 500˚C, resulting in an enhancement of 24%. This is because the relative open structure leads to relatively better flow permeability which increases the heat transfer surface area. Samples made at 700˚C are partly covered with dense CNFs layer and partly with amorphous layer of carbon. Heat transfer enhancement of 34% is achieved which is attributed to the rough surface created by the carbon nano structures.

Keywords *: CNFs, morphology, crystallinity, deposition, enhancement*

1. INTRODUCTION

Micro-scale heat transfer plays an important role in heat removal in many engineering application where space and power density are challenging technological advancements. Some of the application areas are in micro-chips, Micro-electro-mechanical-systems (MEMS) and regenerators (sterling engine and thermo-acoustic heat pumps). The breakthrough discovery of multi wall carbon nanotubes (CNTs)[1] results on novel material which exhibit remarkable mechanical and heat-transport properties, attributed to the strength of the carbon-carbon bond within graphene layers. Nowadays, there is growing evidence, coming from both experimental and theoretical studies that CNTs do indeed have an outstandingly high young's modulus, high thermal stability and thermal conductivity. Due to their extremely high thermal conductivity, carbon nanotubes are considered as a novel material in heat transfer researches [2-5]. The thermal conductivity at room temperature along the axis of the CNTs was found to be greater than 3000W/m.K [6] which results in a substantial improvement of the exchange of heat between the surface and the surrounding fluid flow. In contrary, the thermal conductivity at room temperature of CNTs across the axis (radial direction) is poor with a value of 1.52W/m.K [7]. Consequently, the structural arrangement graphene layers have a tremendous influence on the thermal properties. Carbon nano structures exist in three different graphene arrangement: perfect cylindrical arrangement of graphene sheets (Tubes), conical arrangement of the graphene sheet (fish-bone) and flat graphene arrangement (stacked). These different structures are believed to have different thermal conductivities. Moreover, the thermal conductivities of carbon nano structures is strongly dependent on the degree of crystallinity and presence of impurities. However, qualitative measurement of thermal transport properties of individual fibers remains challenging, due to technological difficulties associated nano-scale experimental measurements[8].

Zhimin Mo et.al [9] reported an effective cooling for microelectronic applications using integrated CNT fins made by lithographic technique and CVD on microchannel surface. It was mentioned that the flow rates were decreased by 12% whereas the heating power input is increased by 23% keeping the transistor temperature 6°C below the reference cooler. It was also suggested that self-aligned CNTs would increase the heat transfer greater than what was achieved. Kordas et.al [10] have reported an efficient chip cooling (about ~1W more power was dissipated) by integrating laser patterned CNT micro fin structures on a silicon chip on 1mm^2 surface compared to bare chip. It was also reported that 11% more power was dissipated during the natural convection and 19% under forced convection. Similar fin structures made up of copper material were investigated for comparison and similar results were obtained. However, an un-patterned CNTs layer shows poor heat transfer performance due to the dense nature of CNTs layer hampered the flow of N_2 in the film limiting the heat transfer only to the upper facet of the films resulting in limited cooling capabilities. It is also suggested that by changing fin geometry, dimension and fin densities more efficient cooling can be achieved.

However, both references lack appropriate method of quantifying the heat transfer with respect to the flow hydrodynamics.

Preliminary experimental research has shown that carbon-nano-fibers deposition on stainless steel foam surface can enhance heat transfer ranging from 30% - 75% while on a carbon foam decreases the heat transfer by 40% [11]. It was explained that the cumulative effect of the an increase of heat exchange surface area, structural arrangement of the graphene layer and higher crystallinity results in the overall performance of the stainless steel foam.

The aim of the present work is to explore the morphological influence of carbon-nano-structured surfaces on heat transfer performance characteristic. The heat transfer performance test was made on 50µm diameter nickel wire by modifying the surface with layer of carbon nano fibers (CNFs) which exhibit different surface morphology and similar graphene layer arrangement. Moreover, the influence of the deposited layer thickness on heat transfer performance is discussed.

2. MATERIALS

Polycrystalline Ni wire (99.9%, Ni270, Alloy Wire International Ltd.), made by wire drawing mechanism, with a uniform diameter of 50µm was used in this study to represent a differential strand of common regenerator element such as metallic foam or wire mesh. The surface of the wire was modified by depositing carbon nano structural layer. High purity gases were used during the synthesis process: hydrogen (99.999%,INDUGAS), nitrogen (99.999% INDUGAS) and ethylene (99.95% PRAXAIR).

3. EXPERIMENT

3.1 CNFs layer synthesis

Three different sample synthesis procedure were designed to obtain different CNFs topological structure. It was designed by indicating three different synthesis temperatures (500˚C, 600˚C and 700˚C). However, samples produced undergoes similar pretreatment in order to have relatively equal number of nucleation sites where carbon nano structures deposit.

Prior to CNF-synthesis, the Nickel micro wire samples were pretreated under reducing atmosphere in a 50mm diameter vertical quartz reactor which was heated from outside by an electrical furnace. The samples were heated to 600˚C with a heating rate of 6˚C/min under nitrogen (inert medium) stream with total flow rate of 100 ml/min. After reaching 600˚C, 30 vol.% hydrogen was introduced in the nitrogen stream to reduce the samples for 1 hr while maintaining the total flow rate at 100 ml/min. Followed by this reduction pretreatment, samples were further brought to the synthesis temperature (500˚C, 600˚C and 700˚C) at a rate of 6˚C/min under nitrogen stream with total flow rate of 100ml/min. The samples were further exposed to a reactive gas mixture of 20 vol.% C_2H_4, 5 vol.% H_2 and 75 vol.% N_2 at 500°C, 600°C and 700°C with total flow rate of 100ml/min. Subsequently, the samples were cooled down in N_2 to room temperature. Finally, samples were further exposed to a jet of air in order to remove the loosely attached carbon nano fibers. The samples synthesized at 500°C, 600°C and 700°C with respect to the synthesis duration will be referred throughout the paper as “5-[time in min]”, “6-[time in min]” and “7-[time in min]” respectively.

3.2 Characterization of CNFs layer

The morphology of the samples was studied with high resolution Scanning Electron microscopy (HR-SEM-LEO-1550) equipped with NORAN EDS and WDS. The average size of the CNFs layer and CNFs diameter was estimated based on 25 observations by post-processed of SEM images using MATLAB. Room temperature Raman spectroscopy, (Bruker optics Senterra Raman microscope spectrometer), was used to evaluate the crystallinity of the CNFs. The sample was analyzed without any sample treatment or preparation.

3.3 Heat transfer measurement setup

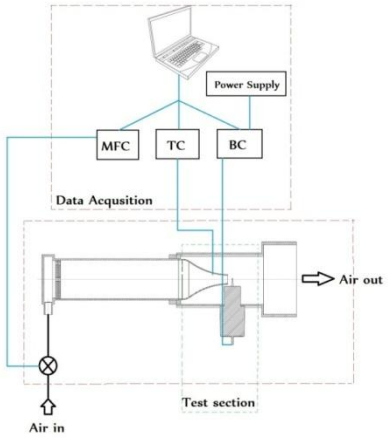

Figure 1 Schematic view of heat transfer measurement setup

The experimental apparatus is divided into two distinct parts: probe calibration and constant temperature (T_w) heat transfer measurement. The schematic diagram of the heat transfer setup is shown in figure 1. Air was supplied from a 6 bar air supply and the flow was controlled by a mass flow controller. The air passes through flow straightener and reaches the nozzle. The nozzle was designed to achieve a constant velocity profile at the exit and the speed (U_∞) was measured by determining the pressure difference over the nozzle using water column. Sample wires were spot welded into a probe and placed perpendicularly facing the flow. The probe was electrically heated to a desired temperature and the temperature of the air flow (T_∞) was measured. The source current (I) was supplied and regulated by high precision DC power supply (Tektronix PWS4205). The amount of voltage drop and the resistance (R_w) were measured using a NI-PCI-6280 module. Film temperature properties such as conductivity(k_f), viscosity(μ_f) and density(ρ_f) are used to process the experimental results. The sample is made up of high

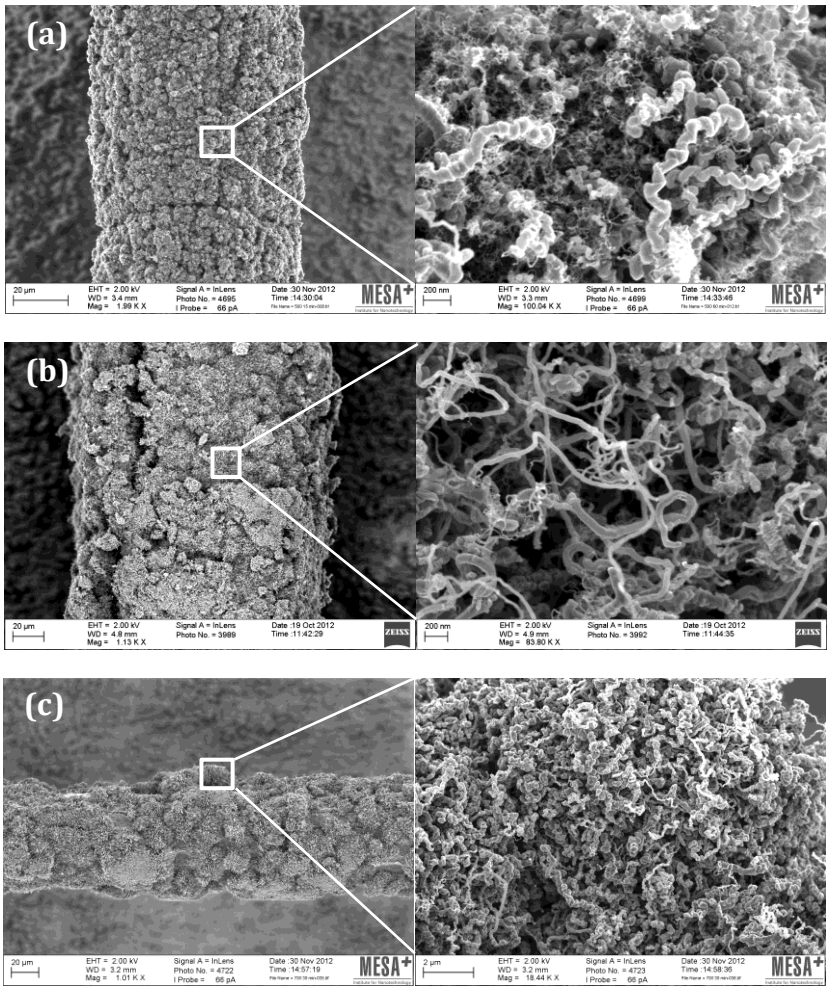

Figure 2 SEM images of surface morphology of CNFs layer produced on 50µm Nickel wire. (a) densely populated CNFs layer grown at 500°C for 1hr which is made up of smaller fibers as small as 8nm diameter entangling larger once (~100nm), (b) CNFs layer produced at 600°C for 1hr with a relatively open CNFs layer, and (c) CNFs layer grown at 700°C for 30min have rougher morphology and open CNFs structures as well.

purity (99.9%Ni) polycrystalline nickel micro wire (Ni270) which is also used as a catalyst and substrate material during the synthesis of the CNF layer. Heat transfer measurement of the bare micro wire (d) was compared with different literatures and satisfactory results were obtained [12].

The porosity and permeability are important parameters to anticipate the amount of flow penetration. Due to the curvature effect of the CNFs covered samples, the porosity and flow permeability increases in the radial direction. This fact creates a region inside CNFs sub-layer where no flow can penetrate. As a result, it is difficult to determine the effective diameter of individual samples made; hence, it affects the heat transfer comparison of each different samples with respect to the flow characteristics. However, the analysis made in this work considers the bare wire diameter as the characteristic diameter of the different sample and the possible range of enhancement that can be achieved by taking the outer diameter of each individual samples in to account is discussed further on.

The Nusselt (Nu_d) and Reynolds (Re_d) number are calculated as:

$$Nu_d = \frac{I^2.R_w}{k_f.\pi.l.(T_w - T_\infty)} \quad (1)$$

$$Re_d = \frac{\rho_f.U_\infty.d}{\mu_f} \quad (2)$$

Heat transfer performance of the modified wire surface are compared and heat transfer enhancement is computed as:

$$\eta = \left[\frac{Nu_{d(CNF)}}{Nu_{d(bare)}} - 1\right] \cdot 100\% \quad (3)$$

Based on the work of Moffat et. al [13], measurement uncertainties are analysed to predict the possible value that an error may have. Based on 120 data samples, results shows that the uncertainty of the measured Nusselt number to be ± 4.4%.

4. RESULTS AND DISCUSSION

4.1 CNFs layer and mechanical stability

CNFs synthesis was achieved on 50µm nickel wire with three different synthesis temperature. The surface morphology proved to be highly dependent on the synthesis temperature. Fig. 2 shows the different morphology attained when carbon deposition occurred at 500°C, 600°C and 700°C. Tip growth of the CNFs is observed on all the synthesis conditions. Different CNFs layer thicknesses, ranging from 1 µm to 59 µm, is made to investigate the influence of layer thickness of different CNFs layer morphologies on heat transfer characteristics, see Fig.3. The thickness of the layer is dependent on the synthesis duration and temperature.

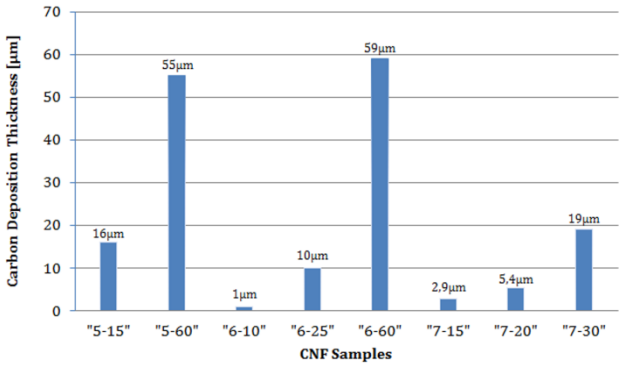

Figure 3 Carbon deposition thickness for different synthesis duration.

The mechanical stability of the layer is directly related to the morphology and structural make up of individual fibers. Samples produced at 600°C (Fig.2-b) can be easily destroyed while handling the samples. However, almost equally sized sample produced at 500°C (Fig.2-a) have better mechanical stability when it is handled. This is because the open structural nature of the samples and the density of the carbon layer.

4.2 Influence of surface morphology on heat transfer performance

4.2.1 Surface characterization

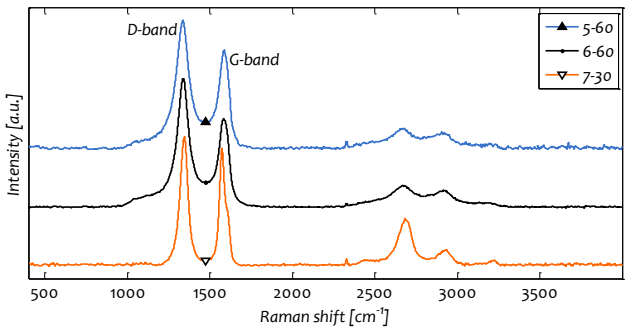

Figure 4 Raman spectra of CNFs with different synthesis conditions

To study the influence of surface morphology of the carbon layer on heat transfer, three samples with different surface morphology are selected. The CNFs layer thickness on average 55µm, 59µm and 19µm for growth temperature of 500°C, 600°C and 700°C respectively, see table 1. However, the range of diameter of the individual fibers is different for the three samples. The average diameter increased with synthesis temperature. SEM image shows that the '5-60' sample is made up of large strand of fibers (~120nm) entangled with small fibers (as small as 8nm) which increases the density of the fibers population. Sample '6-60' shows relatively open CNF morphology, compared to the '5-60', with fibers diameter ranging from 30nm to 120nm, see Fig. 2-a and 2-b. Sample '5-60' and '6-60' are entirely covered with CNFs layer while '7-30' is partly covered with fibers and partly with amorphous layer of carbon (Fig.2-c). The layer density of the CNFs layer was compared among the samples with weight of carbon deposit per deposit layer thickness. The amount of carbon deposited on sample '5-60' is ~85% larger than sample '6-60' while the layer thickness of the '5-60' is ~7% less than sample '6-60'. This supports the previous argument made from the SEM image. However, '7-30' results shows an entirely different CNFs layer morphology compared to the '5-60' and '6-60'. Sample '7-30' exhibit larger fiber diameter, as thick as 200nm, and relatively large amount of carbon deposit per CNFs layer thickness, see Table 1. This Similar to other non-metallic materials, the transport of thermal energy in carbon nano fibers or tubes is assumed to occur via phonon conduction mechanism. The phonon conduction in these structures is influenced by several processes such as the number of phonon active modes, the boundary surface scattering, the length of the free path for the phonons and inelastic Umklaap-scattering (an anharmonic phonon-phonon or electron phonon scattering process)[14,15]. The thermal conductivity of the carbon nano structures is dependent on how the graphene structural are arrangement, the diameter and the length of the filaments, the number of structural defects and morphology, and on the presence of impurities [16-18].

Table 1 Carbon nanofibers structural characteristics

Sam-ples	layer thickness [µm]	Fiber-diameter -range (avg.) [nm]	carbon deposit [g_C/g_{Ni}]	D band [cm^{-1}]	G band [cm^{-1}]	I_D/I_G
5-60	~55	8-120 (20)	~0.237	1335	1586	1.301
6-60	~59	30-120 (60)	~0.128	1336	1583	1.457
7-30	~19	80-200 (120)	~0.302	1345	1572	1.099

The crystallinity of the CNFs layer is believed to have a great influence on the thermal conductivity of the material due to the graphene layer arrangement [6,7]. So as to measure the degree of structural order of materials, Raman spectroscopy was applied. The Raman spectra of CNF layer synthesized on Ni wire is featured D and G bands which is typical for carbon nano structures, see Fig 4. Two clear bands are visible for all samples, centered between ~1335 and ~1586 cm^{-1}. It is known that the

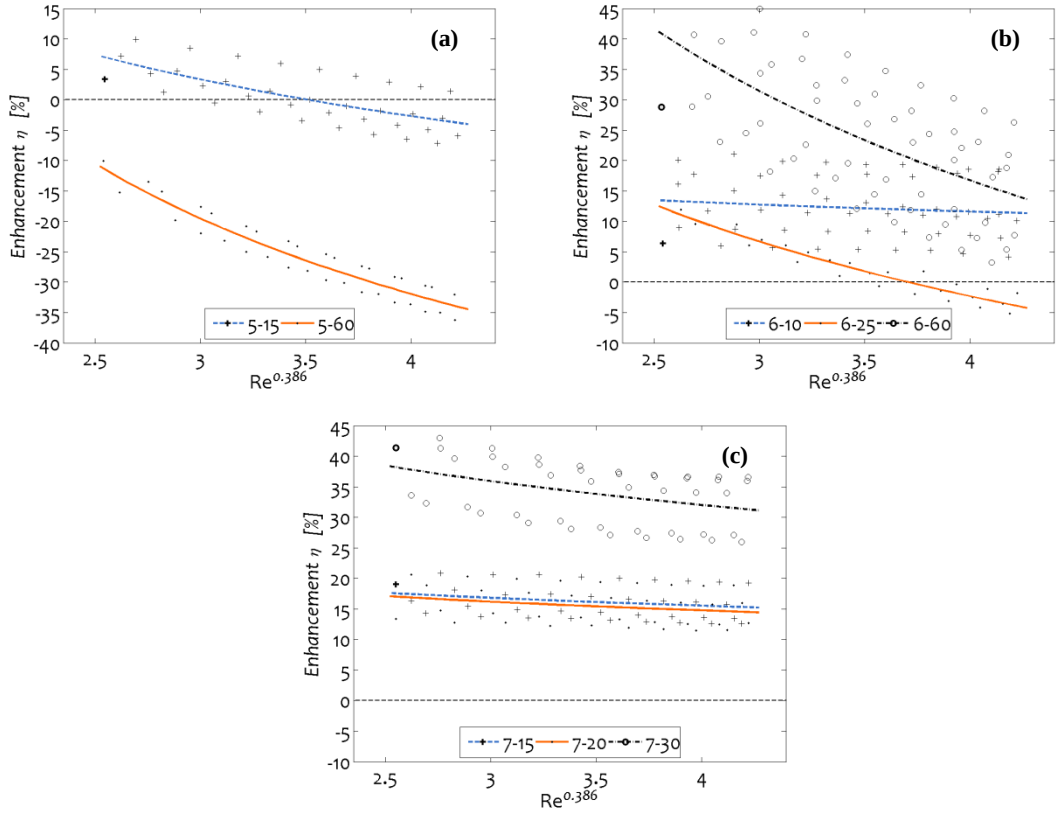

Figure 5 Heat transfer performance characteristic of 50µm diameter nickel wire covered with CNFs layer produced at (a) 500°C with relatively dense structural morphology, (b) 600°C with relatively open structural morphology and (c) 700°C with rough structural morphology.(In all cases, bare wire diameter is used as characteristic diameter).

Raman spectrum of single-crystal graphite, as well as of highly oriented pyrolytic graphite (HOPG) have a single band at ~1582 cm^{-1} (G-band), which is known as graphite mode. Carbon materials with less order of crystallinity exhibit a band at ~1350 cm^{-1}, which is a defect induced Raman band named as the defect mode (D-band) [19, 20]. The ratio of the relative intensity of the D-band and G-band (I_D/I_G) can be utilized to assess the degree of graphitization and the alignment of the graphene planes. As a result, the relative intensity ratio can help in comparing the relative conductivity difference that could exist among the samples made.

The relative intensity ratio (I_D/I_G) of '5-60', '6-60' and '7-30' are 1.301, 1.457 and 1.099 respectively. The smaller the relative intensity ratio of the carbon nano structures, the more ordered (less defect) and more crystalline layer carbon nano structures it has. Sample '5-60'and '6-60' have almost the same D-band and G-band. In addition, the intensity ratio difference, among the two samples, is relatively small when it is compared to '7-30'. As a result, '5-60' and '6-60' are believed to have similar thermal conductivity than '7-30'. However, due to its lower relative intensity ratio (I_D/I_G), sample '7-30' is relatively more crystalline and highly ordered than '5-60' and '6-60'. As a result, the thermal conductivity of the CNFs sample can be rated as '7-30' > '5-60' ≥ '6-60'.

4.2.2 Heat transfer results

In this section, the different surface morphologies are discussed for their heat transfer performance. Fig.2 shows that sample '5-60' and '6-60' have more comparable surface structure than sample '7-30'. Both sample '5-60' and '6-60' are made up of thick layer of CNFs with different size of structural openings and almost similar conductive layer. However, the heat transfer performance of sample '5-60' is on average 26% less than the bare wire whereas sample '6-60' have on average a positive heat transfer enhancement of 24%, see Fig.5-a,b. However, sample '6-60' shows large scattering in the data (Fig.5-b) which arises from the mechanical instability of the CNFs layer, when handled, while samples '5-60' are relatively stable (Fig.5-a). Further investigation shows that removing the layer of carbon nano structures results in similar heat transfer performance as the bare wire (results not shown here). As a result, the CNFs sample performance of '6-60' is attributed to the relative large structural openings of sample and have better flow permeability (Fig.2-b) which increases the heat exchange surface area. Conversely, sample '5-60' is anticipated to have less flow permeability and hence air trapped inside the structure creates an insulating effect.

Sample '7-30' shows an entirely different surface morphology (see Fig.2-c) with higher degree of crystallinity (see

table 1) of the carbon nano structures and relatively closed structures. An exceptional heat enhancement (see Fig.5-c) of 34% is achieved by sample ‘7-30’. Though the heat transfer enhancement of samples made at 500°C and 600°C is explained with their relative structural openings and flow penetration, the performance of sample ‘7-30’ is attributed to the combined effect of rough and conductive layer of carbon nanofibers which disturbs the flow boundaries across the wire and increase surface area for heat transfer.

4.3 Influence of CNFs layer thickness on heat transfer performance

In this section, the previously discussed samples are studied for their influence on heat transfer when subjected to different synthesis time. The carbon deposit layer thickness of each sample is measured. Since the samples are covered with porous layer of carbon, it is difficult to determine the effective diameter of each sample where no flow penetration exists. This influences the Nusselt number comparison due to the shift of the Reynolds number for different samples. Fig.6 compares the performance enhancement in heat transfer for the inner most (50µm) diameter with the outer most diameter for each samples.

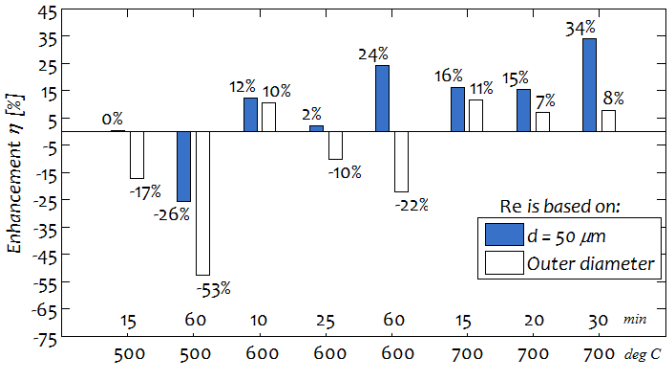

Figure 6 Overall performance evaluation of the CNFs samples with comparisons of characteristic diameter of the bare wire (50µm) and outer most diameter of each samples.

Fig.3a shows that samples, which are synthesized at 500°C, with 16µm layer thickness have better heat transfer enhancement than the 55µm samples. This is strengthening our expectation of the air pockets trapped inside the impermeable CNFs layer. However, samples produced at 600°C did not show a trend of increasing the thickness would increase the heat transfer anticipation. Heat transfer is enhanced for 1µm layer thickness while it decreases for 10µm thickness and further increases for the 59µm thick layer of CNFs. Samples produced at 700°C shows almost similar performance at 2.785µm and 5.5µm layer thickness. However, a 19µm thick layer shows better heat transfer enhancement.

It is strongly believed that the difference on heat transfer pattern exists due to the amorphous carbon layer thickness which plays a significant role in reducing the heat transfer. However, further investigation should be done to understand these results by looking in depth to the sub-layer of the deposit.

5. CONCLUSIONS

Carbon nano fibers were grown on a 50µm nickel wire using CVD method at different growth parameters. Both the influence of morphology and CNFs layer thickness is studied. Different surface morphology was successfully obtained with similar graphitic behavior which helps to investigate their influence on heat transfer. Lower heat transfer performance was achieved for the ‘5-60’ due to the dense CNFs layer morphology while heat transfer enhancement was achieved for the ‘6-60’. High heat transfer performance of ‘6-60’ (24%) compared to ‘5-60’(-26%) is explained by the fact that less dense and open structure which acquires better flow permeability, hence better heat exchange. The different morphology of the sample ‘7-30’ helped to attain heat transfer enhancement of 34%, attributed to the combined effect of rough and conductive layer of carbon nanofibers which disturbs the flow boundaries across the wire and increase surface area for heat transfer.

REFERENCES

1. Iijima S Helical microtubes of graphitic carbon Nature **354**,56-58,1991.
2. Min-Sheng Liu, Mark Ching-Cheng Lin, I-Te Huang and Chi-Chuan Wang Enhancement of thermal conductivity with carbon nanotubes for nanofluids International Communications in Heat and Mass Transfer **32** 1202–10,2005.
3. Ki-Jung Park and Dongsoo Jung Enhancement of nucleate boiling heat transfer using carbon nanotubes International Journal of Heat and Mass Transfer **50** 4499–502,2007.
4. Launay S, Fedorov A G, Joshi Y, Cao A, Ajayan PM Hybrid micro-nano structured thermal interfaces for pool boiling heat transfer enhancement Microelectronics Journal **37** 1158–64,2006.
5. Zhen-Hua Liu and Liang Liao Forced convective flow and heat transfer characteristics of aqueous drag-reducing fluid with carbon nanotubes added International Journal of Thermal Sciences **49**,2331-38,2010.
6. Kim P, Shi M L and McEuen Thermal Transport Measurements of Individual Multiwalled Nanotubes Phys. Rev. Lett. **87** 215502-04,2001.
7. Sinha Saion , Barjami Saimir, Iannacchione Germano, Schwab Alexander and Muench George Off-axis thermal properties of carbon nanotube films. Journal of Nanoparticle Research **7** (6) 651–7,2005.
8. Xie H, Cai A, Wang X. Thermal diffusivity and conductivity of Multiwalled carbon nanotube arrays.Phys Lett A;**369**:120-123, 2007
9. Zhimin Mo, Raluca Morjan, Johan Anderson, Eleanor E.B. Campbell and Johan Liu Integrated nanotube micro cooler for microelectronics applications Electronic components and technology conference 51-4,2005.
10. Kordas K, Toth G, Moilnen P, Kumpumaki M and van Hakangas J Chip cooling with integrated carbon

nanotube microfin architectures Appl.Phys.Lett. **90** 123105,2007.

11. Fahong Li, Leon Lefferts and Theo H. van der Meer, Study on Heat Transfer Enhancement by Metallic Foams with Carbon Nano Fibers (CNFs) 6th World Conference on Experimental Heat Transfer, Fluid Mechanics, and Thermodynamics (Matsushima, Miyagi, Japan) 17-21,2005.
12. Taha T.J., Thakur D.B. and Van der Meer T.H. Towards convective heat transfer enhancement: surface modification, characterization and measurement techniques *J. Phys.: Conf. Ser*. **395** 012113,2012.
13. Moffat R.J. Describing the uncertainities in experimental results Experimental Thermal and Fluid Science **1**(1) 3-17,1988
14. Maultzsch J., S. Reich, C. Thomsen, E. Dobardžić, I. Milošević, M. Damnjanović Phonon dispersion of carbon nanotubes Solid State Commun, **121**, pp. 471–474, 2002
15. Ishii H., Kobayashi N., Hirose K. Electron–phonon coupling effect on quantum transport in carbon nanotubes using time-dependent wave-packet approach Physica E, **40**, pp. 249–252, 2007
16. Maeda T., Horie C. Phonon modes in single-wall nanotubes with a small diameter Physica B, **263–264**, pp. 479–481, 1999
17. Kasuya A., Saito Y., Sasaki Y., Fukushima M., Maeda T., Horie C., Nishina Y. Size dependent characteristics of single wall carbon nanotubes Mater Sci Eng A, 217/218, pp. 46–47, 1996
18. Popov V.N. Theoretical evidence for T1/2 specific heat behavior in carbon nanotube systems Carbon, **42**, pp. 991–995, 2004
19. Endo M, Nishimura K, Kim Y A, Hakamada K, Matushita T, Dresselhaus M S and Dresselhaus G Raman spectroscopic characterization of submicron vapor-grown carbon fibers and carbon nanofibers obtained by pyrolyzing hydrocarbons Journal of Materials Research **14** 4474-77,1999.
20. Kim C, Park S H, Cho J K, Lee D Y, Park T J, Lee W J and Yang K S Raman spectroscopic evaluation of polyacrylonitrile-based carbon nanofibers prepared by electrospinning Journal of Raman Spectroscopy **35** 928-33, 2004.